nature ecology & evolution

ARTICLES

PUBLISHED: 8 MAY 2017 | VOLUME: 1 | ARTICLE NUMBER: 0153

Direct observation of increasing recovery length before collapse of a marine benthic ecosystem

Luca Rindi[1]*, Martina Dal Bello[1†], Lei Dai[2‡], Jeff Gore[2] and Lisandro Benedetti-Cecchi[1]

Ecosystems can experience catastrophic transitions to alternative states, yet recent results have suggested that slowing down in rates of recovery after a perturbation may provide advance warning that a critical transition is approaching. Perturbation experiments with microbial populations have supported this hypothesis under controlled laboratory conditions, but evidence from natural ecosystems remains rare. Here, we manipulated rocky intertidal canopy algae to test the hypothesis that the spatial scale at which the system recovers from a perturbation in space should increase as the system approaches the tipping point, marking the transition from a canopy-dominated to a turf-dominated state. Empirical estimates of recovery length, a recently proposed spatial indicator of an approaching tipping point, were obtained by comparing the spatial scale at which algal turfs propagated into canopy-degraded regions with decreasing canopy cover. We show that recovery length increased along the gradient in canopy degradation, providing field-based evidence of spatial signatures of critical slowing down in natural conditions.

Ecological shifts are increasingly observed in natural systems as diverse as shallow lakes, coral reefs and savannahs[1–3]. The ubiquity of such phenomena has stimulated research on early warning signals to forewarn the approach of a system to a tipping point[4]. There is a growing interest in using the phenomenon of 'critical slowing down' to measure the distance of a system to a critical threshold[5,6]. According to theory, a system that is approaching a critical threshold recovers more slowly from perturbations and may experience a change in the pattern of fluctuations[4,5,7]. This phenomenon may also be signalled by generic indicators of an approaching tipping point, such as increasing variance and autocorrelation of state variables. Critical slowing down and early warning signals have been evaluated using correlative approaches (for example, through the analysis of time series and spatial data), simulations and experiments[8–15].

The phenomenon of critical slowing down and its related signatures are expected to emerge before a wide range of transitions in complex systems[16,17]. Previous research into critical slowing down has largely focused on the use of time series to predict the proximity of a system to a tipping point[11,14,18,19]. However, early warning signals derived from time series require high-quality observations over a long time span, which are often difficult to obtain[20]. An alternative approach involves the development of spatial early warning signals[21–23]. Critical transitions in spatially extended ecosystems may be announced by enhanced spatial variance and autocorrelation and by 'reddening' in the power spectrum of the state variable[24–26]. Moreover, several studies have shown how changes in spatial patterns could provide signatures of impending transitions in spatially organized ecosystems[27–29]. However, some spatial patterns are determined by the particular processes involved (for example, spatial self organization) and consequently cannot be extended to other ecosystems[30].

A novel spatial indicator that has been proposed[31], the recovery length, is defined as the spatial distance from a perturbation at which a population recovers. The spatial scale of recovery in connected yeast populations was shown to be increased close to the tipping point[31]. Although such manipulations of synthetic communities have advanced our understanding of regime shifts considerably, most empirical tests of early warning signals have focused on single species in almost noise-free laboratory conditions[9,31,32]. Therefore, the current challenge is to extend this test to spatially extended multispecies systems that experience natural fluctuations, a crucial step before we can apply the proposed indicator in environmental conservation and management[33].

Here, we use a rocky intertidal system characterized by two alternative states, one dominated by macroalgal canopies (*Cystoseira amentacea* Bory var. *stricta* Montagne) and one by turf-forming algae (low-lying filamentous and other very small algae) to evaluate recovery length as a spatial early warning indicator of an approaching tipping point[31] (Supplementary Fig. 1).

Results

On the basis of the results of a previous experiment, we expected *C. amentacea* and the associated understory assemblages to undergo a regime shift that leads to turf-dominated state, when canopy cover is progressively reduced[10]. To test this hypothesis in a spatial context, we performed a spatially uniform canopy removal experiment and measured the percentage cover of algal turfs over the following two years (see Methods). We then used potential analysis[34] to construct potential landscapes and infer stable and unstable equilibria for different levels of canopy degradation. This analysis assumes that the frequency distribution of the state variable (algal turf cover) is shaped by the interaction between the deterministic dynamics (canopy removal) and stochastic forces (for example, sea storms, topography of the substratum). As a consequence of stochastic perturbations, a system exhibiting bistability may 'flicker' between alternative states, resulting in a potential landscape with two minima (stable states) separated by a local maximum (unstable equilibrium) (Supplementary Fig. 2). Using this approach, we found that turf cover showed a single low-value equilibrium at low levels of canopy removal (0–33%) (Fig. 1a). By contrast, at intermediate levels of canopy degradation (33–70%),

[1]Department of Biology, University of Pisa, CoNISMa, Via Derna 1, Pisa 56126, Italy. [2]Physics of Living Systems, Department of Physics, Massachusetts Institute of Technology, 400 Technology Square, NE46-609, Cambridge, Massachusetts 02139, USA. †Present address: Physics of Living Systems, Department of Physics, Massachusetts Institute of Technology, 400 Technology Square, NE46-609, Cambridge, Massachusetts 02139, USA. ‡Present address: Department of Ecology and Evolutionary Biology, University of California, Los Angeles, California 90095, USA. *e-mail: lrindi@biologia.unipi.it

© 2017 Macmillan Publishers Limited, part of Springer Nature. All rights reserved.

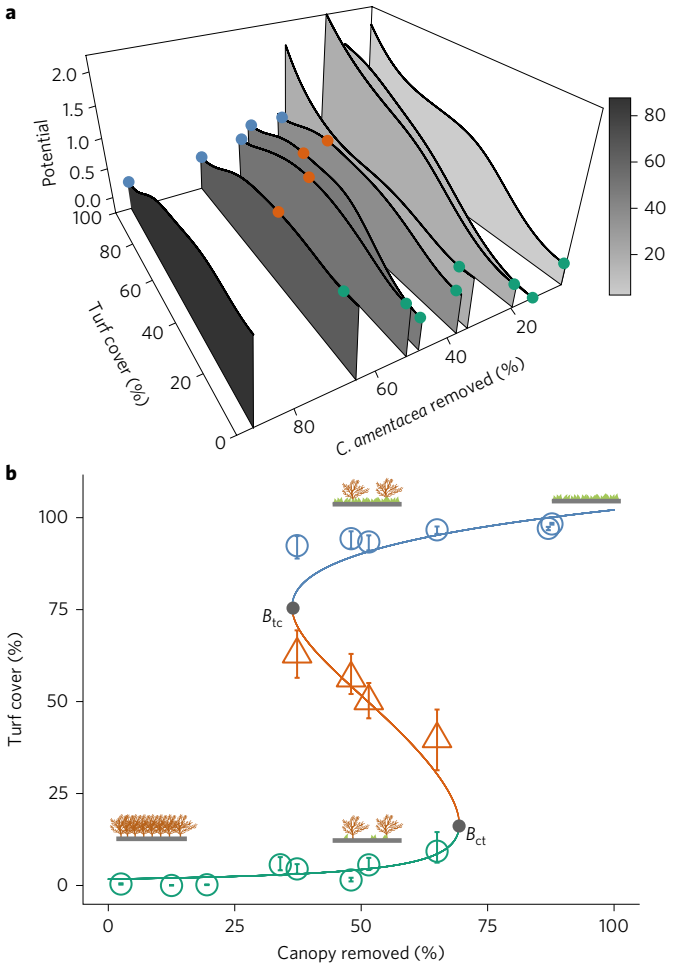

Figure 1 | Canopy degradation leads to a regime shift from a canopy- to a turf-dominated state. a, Potential landscapes inferred from experimental data (see Methods). The balls mark the minima and maxima of the potential landscapes corresponding to the canopy- (green) and the turf-dominated (blue) states, whereas unstable points are shown in orange. Grey colours indicate the percentage cover of canopy removed (expressed as 100 minus the percentage of observed canopy cover). **b**, The stable and unstable equilibria of algal turfs as a function of canopy removed. The transition from a canopy- to a turf-dominated state occurs at about 70% of canopy degradation (indicated as B_{ct}), whereas the transition from a turf- to a canopy-dominated system occurs at about 40% of canopy loss (B_{tc}). Lines represent the fit of the *Cystoseira*–turf model: stable equilibria of the canopy- and turf-dominated systems are indicated in blue and green, respectively, whereas unstable equilibria are shown in red. Error bars are bootstrapped 95% confidences intervals. Cartoons illustrate the two alternative states: *Cystoseira amentacea* in brown and algal turfs in green.

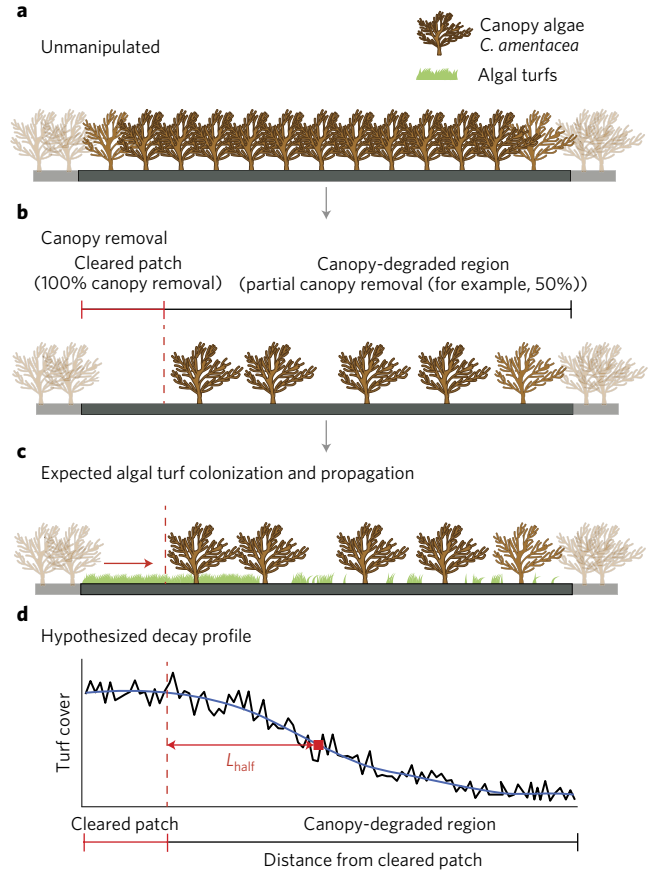

Figure 2 | Schematic illustration of the experiment and measurement of the recovery length. a, Horizontal view of an unmanipulated transect with full cover of *C. amentacea* (semi-transparent plants indicate that the canopy extended off the first two quadrats; approximately 90 cm). A cleared patch where all erect organisms were cleared from the substratum was produced at the edge of each transect to facilitate the colonization of algal turfs. **b**, Example of a canopy removal transect where approximately 50% of *C. amentacea* was removed. **c**, The algal turfs (in green) colonizing the cleared patch were expected to propagate into the canopy-degraded region. **d**, Hypothesized distance–decay profile of turf cover. As the distance from the low quality patch increases, the cover of algal turf should gradually decline to zero. Recovery length is defined as the spatial distance from the edge of the cleared patch (dashed line) at which the system becomes free from algal turf. The L_{half} (red square) marks the position of the half recovery point.

algal cover showed a bistable pattern, with one state dominated by algal turfs and the other dominated by the algal canopy (Fig. 1a and Supplementary Fig. 2). As canopy cover was progressively reduced, the size of the basin of attraction around the canopy-dominated state shrunk, whereas that of the turf-dominated state increased (Fig. 1a,b, B_{ct}). When more than 70% of the canopy was removed the system shifted to the turf-dominated state displaying only one basin of attraction (Fig. 1b, B_{ct}). A simple mathematical model parameterized by these data indicated the presence of a tipping-point at approximately 70% of canopy removal, beyond which the system shifted to the turf-dominated state (Fig. 1b, B_{ct}).

When approaching a tipping point, we expected the canopy-dominated state to become more susceptible to spatial perturbations[31]. In our reconstructed stability landscapes, loss of resilience occurs as the basin of attraction around the canopy-dominated state shrinks (Fig. 1a,b). As the tipping point approaches, the ability of algal turfs to penetrate into areas occupied by *C. amentacea* should increase as the system loses stability (Fig. 2). To experimentally test this prediction, we performed a field experiment in which we evaluated the ability of stands of *C. amentacea* to prevent the propagation of algal turfs from patches with no canopy, which acted as a source for diffusing turf species, to a canopy-degraded region. We established eight experimental transects of seven contiguous quadrats each, in areas originally covered by *C. amentacea* (Fig. 2a). In each experimental transect, two regions of different quality were produced: a patch where all *C. amentacea* was completely removed (hereafter, cleared patch), and a canopy-degraded region which was allocated to each of the following treatments: 0%, 25%, 50% and 75% canopy removal (hereafter, canopy-degraded region, Fig. 2b). We evaluated the colonization success of algal turfs by estimating their percentage cover along the gradient of canopy degradation. The percentage cover of algal turfs was assessed twice: after one and two years following the set-up of the experiment. To capture

© 2017 Macmillan Publishers Limited, part of Springer Nature. All rights reserved.

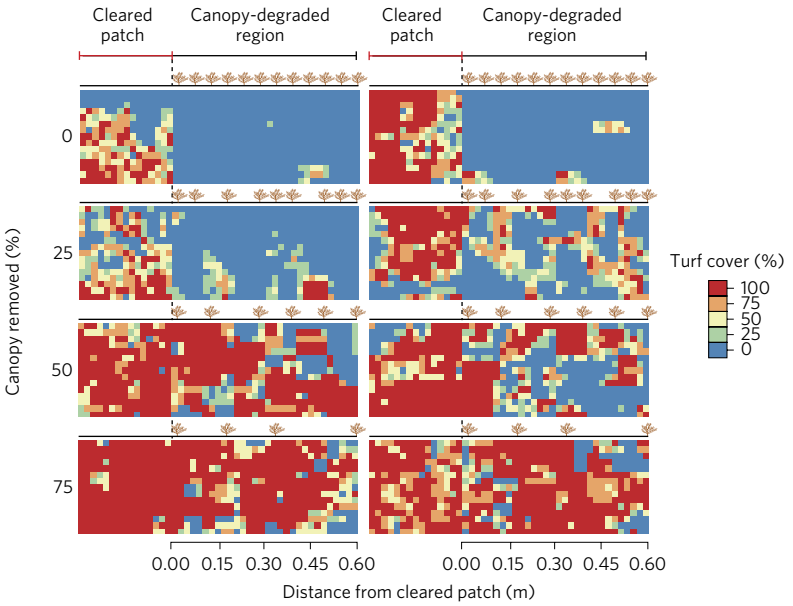

Figure 3 | Canopy degradation enhanced the propagation of algal turfs into the experimental transects. Heat maps were generated using final turf cover data from two replicated transects for each level of canopy removal (0%, 25%, 50% and 75%). Similar results were obtained with data from the first sampling year (Supplementary Fig. 3). The vertical dashed lines separate the cleared patch on the left from the first two adjacent quadrats of a transect on the right.

the propagation of algal turfs from the cleared patch to the canopy-degraded region, we sampled each transect at high spatial resolution (see Methods). We expected that algal turfs would completely colonize the cleared plots and have variable success in propagating vegetatively into the canopy-degraded region, depending upon the amount of canopy removed (Fig. 2c,d).

Consistent with this expectation, our experimental results showed that the increase in canopy degradation led to a deeper propagation of algal turfs from the cleared patch into the canopy-degraded region in both sampling years (Fig. 3 and Supplementary Fig. 3). In control transects (0% of canopy removed), a sharp boundary of algal canopies prevented the propagation of algal turfs from the cleared patch into the transect. As the amount of canopy removed in the canopy-degraded region increased, the system progressively lost the capacity to prevent algal turf propagation from the cleared patch. In particular, in the 50% and 75% canopy removal treatments, algal turfs propagated much further from the cleared patch (Fig. 3).

To further test the hypothesis that the spatial scale at which the percentage cover of algal turfs decays to zero should increase as the system approaches the canopy threshold, we developed a spatial version of the canopy–turf model (see Methods). This model reflects the two-dimensional spatial structure of experimental transects and explicitly includes the heterogeneity in spatial distribution of *C. amentacea*. Model simulations supported our hypothesis and the experimental observation that the spatial scale at which algal turf propagates within the higher quality region increases with canopy loss (Fig. 4a,b and Supplementary Fig. 4).

To quantify the spatial scale at which algal turfs propagated into the canopy-degraded region we used two different metrics of recovery length: the half-point recovery length (L_{half}) and the exponential recovery length (L_{exp})[31]. We quantified both indicators by computing the one-dimensional normalized decay profile for each experimental transect (see Methods). The one-dimensional decay profiles (Fig. 5a) showed spatial patterns that were consistent with two-dimensional data (Fig. 3 and Supplementary Figs 3, 5). The L_{half} measures the distance between a cleared patch and the spatial location at which the percentage cover of algal turfs halves (Fig. 2d). We estimated L_{half} by fitting a local polynomial regression to the one-dimensional decay profiles of each experimental transect (Fig. 5a,b and Supplementary Fig. 5). The L_{exp} was obtained by fitting an exponential function to the decay profile of each transect (Supplementary Fig. 6). The half-point recovery length increased more than four-fold along the gradient of canopy degradation (Fig. 5c). This result was unaffected by a particular choice of the size of the spanning window used in smoothing the data (Supplementary Fig. 7 and Supplementary Methods). The L_{exp} more than doubled along the gradient of canopy degradation (Fig. 5d), showing the same pattern of an increasing L_{half}. These results were supported by spatial model simulations, which showed a consistent increase of both L_{half} and L_{exp} along the gradient of canopy degradation (Fig. 4c).

Discussion

Our results show that recovery length may anticipate the critical threshold marking the transition between the canopy- to the turf-dominated state. In particular, both metrics for the recovery length, L_{half} and L_{exp}, increased markedly along the gradient of canopy degradation. These findings highlight the potential of applying spatial indicators for loss of resilience to forewarn the approach of a system to a critical threshold. Notably, the recovery length can, in principle, be measured at any particular moment in time; the only requirement is the presence of a sharp boundary in external conditions (canopy cover in our case) between regions of different quality. Such boundaries are present at a variety of spatial scales in aquatic and terrestrial ecosystems. For example, small-scale (hundreds of centimetres to tens of metres) boundaries and sharp habitat transitions have been documented in algal canopies[35], mussel beds[36], shallow lakes[37], salt marshes[38] and forest–savannah[39]. These are appropriate systems to further test the ability of the recovery length to inform on impending regime shifts in real-world conditions.

Previous work has shown how generic temporal and spatial indicators can successfully indicate the approaching shift between contrasting trophic structures in a lake ecosystem[11,12,40]. However, early warning signals, such as spatial correlation and spatial variance, may fail to show the approach to a tipping point in systems in which scale-dependent feedbacks generate periodic spatial patterns[21,30]. In contrast to patch-based and pattern-based indicators (for example, patch size distribution and regular-periodic patterns)[27,41,42],

© 2017 Macmillan Publishers Limited, part of Springer Nature. All rights reserved.

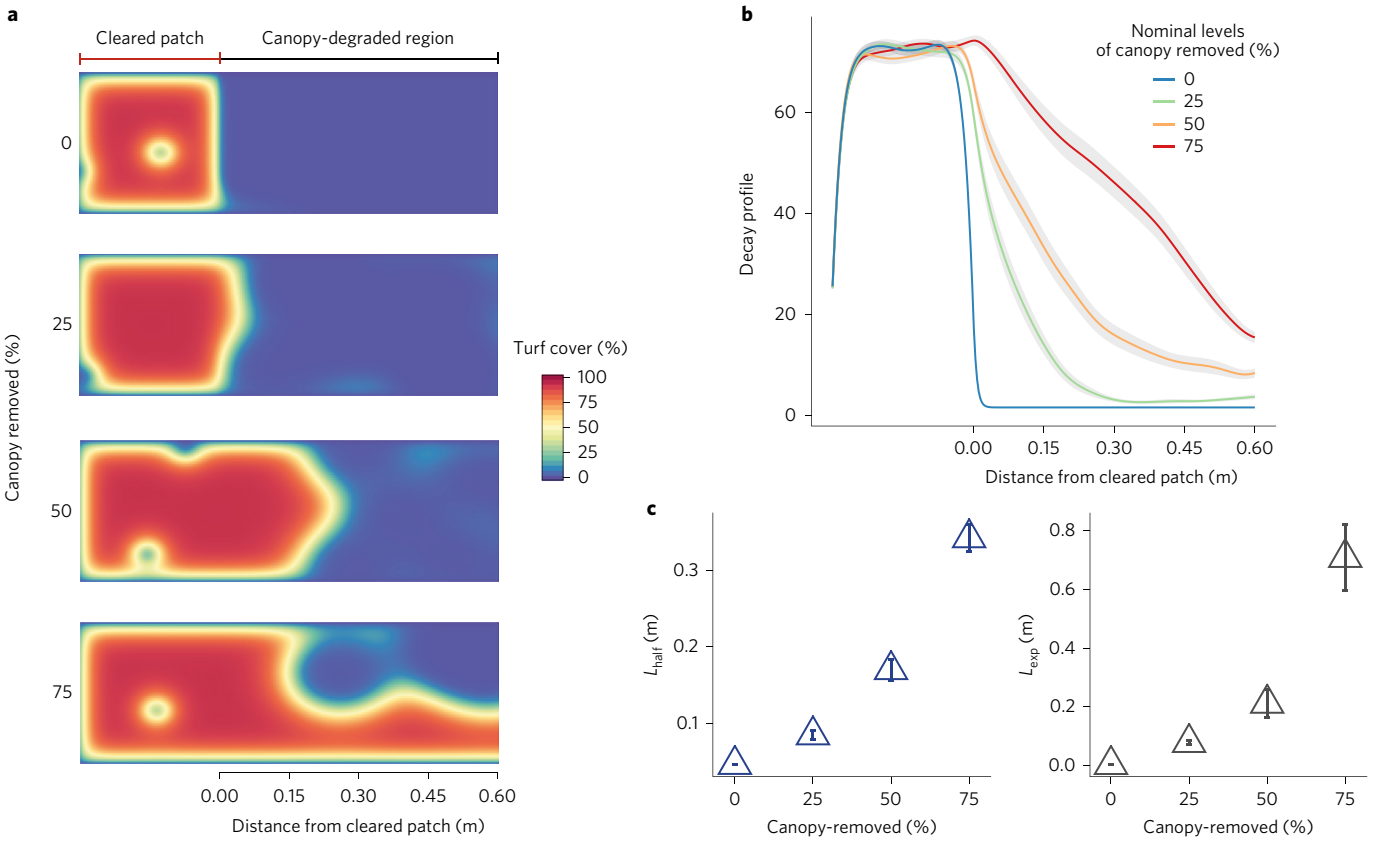

Figure 4 | Simulations of the spatial version of turf–*Cystoseira* model show an increase in the spatial scale of turf propagation along a gradient of canopy degradation. a, The heat maps show the spatial distribution of turf cover at 0%, 25%, 50% and 75% of canopy removal. The percentage of algal turfs is colour coded. **b**, Simulated averaged decay profiles for different levels of canopy removed. The shaded regions correspond to the standard errors of 100 simulations. **c**, Half-point recovery length (L_{half}) and exponential recovery length (L_{exp}). Data are the means ± s.e.m. over 100 simulations.

recovery length metrics may be applied to a wider range of spatial systems given that the recovery of local patches slows down when approaching a tipping point. Simulations have also shown that recovery length may be less data demanding compared to more traditional indicators[31]. However, the recovery length may not be suitable for the identification of an approaching tipping point in highly spatially heterogeneous systems, where strong heterogeneity (for example, the alternation of favourable and unfavourable abiotic conditions) in the landscape may alter the diffusion patterns across space. Strong spatial heterogeneity may hamper the ability of recovery length and other spatial indicators (for example, spatial correlation) to provide early warning of upcoming transitions[22,23,31]. Therefore, the judicious use of all available indicators will provide the best way to evaluate potential impending regime shifts in practical applications.

Canopy algae such as kelps and fucoids are dominant habitat-forming species in rocky intertidal and shallow subtidal habitats along the world's temperate coasts[43]. There is increasing concern about the ongoing replacement of structurally complex algal canopies by less complex habitats that are dominated by turf-forming species or barren grounds, ultimately resulting in the loss of ecosystem services[44–46]. Consideration of recovery length in environmental sampling could substantially contribute to identify areas that are prone to the transition to a degraded state and may help prioritizing management efforts and economic investments for the conservation of endangered marine ecosystems[47]. Given the concern that increasing human pressure can lead to pronounced shifts in many natural and social systems[48–50], the capacity to obtain snapshot measurements of resilience must become a priority for environmental conservation and management.

Methods

Study system. The experiment was initiated in July 2013 at Capraia Island (43.048° N, 9.828° E), about 64 km off the Western coast of Italy, in the Ligurian Sea (north-west Mediterranean). At heights on the shore between 0 and −0.3 m with respect to the mean low water level, canopy algae *Cystoseira amentacea* Bory var. *stricta* (Montagne) forms belts extending for tens of meters in the alongshore direction. *C. amentacea* maintains a species-rich understory assemblage of small algae and sessile invertebrates[44]. This interaction is typically described as a facilitation: the canopy provides shade and ameliorates physical stress for understory species and it also prevents the settlement of algal turfs[51]. The canopy dominated state is stable, because it prevents the settlement and expansion of algal turf[52]. Algal turfs are an intricate mat of low-production and low-diversified tiny algae, that can spread vegetatively and recruit as propagules from the water column[53]. Once established, algal turfs develop in a dense mat that prevents the settlement of *C. amentacea*[44,52] (Supplementary Fig. 1).

Experimental design. In July 2013, we established 8 transects of six 30 × 30 cm contiguous quadrats in areas fully covered by *C. amentacea* (100%). Two replicate transects were randomly assigned to each of the following treatments: canopy control (0% canopy removal), 25%, 50% and 75% of canopy removal. Fronds and holdfasts of *C. amentacea* were removed by hammer and chisel, paying care not to damage the understory assemblages. A cleared patch of 30 × 30 cm, where all *C. amentacea* was completely removed (including understory assemblages), was produced at one end of each transect (Fig. 2b). Treatment conditions were maintained throughout the duration of the study by keeping the percentage cover of *C. amentacea* as close as possible to the nominal level in each experimental transect.

Sampling. The response of algal turfs and *C. amentacea* to experimental treatments was evaluated twice: one and two years after the set-up of the experiment (July 2014, July 2015). Visual estimates of percentage cover were used to assess the abundance of algal turf in each of the 30 × 30 cm plots along the transects. The cleared patch and the first two adjacent quadrats of the nearby transect were sampled by dividing each of the 30 × 30 cm plots into a grid of 15 × 15 sub-quadrats of 2 × 2 cm, yielding 675 observations for each of the transects with cleared patches. We focused on the cleared patch and the

© 2017 Macmillan Publishers Limited, part of Springer Nature. All rights reserved.

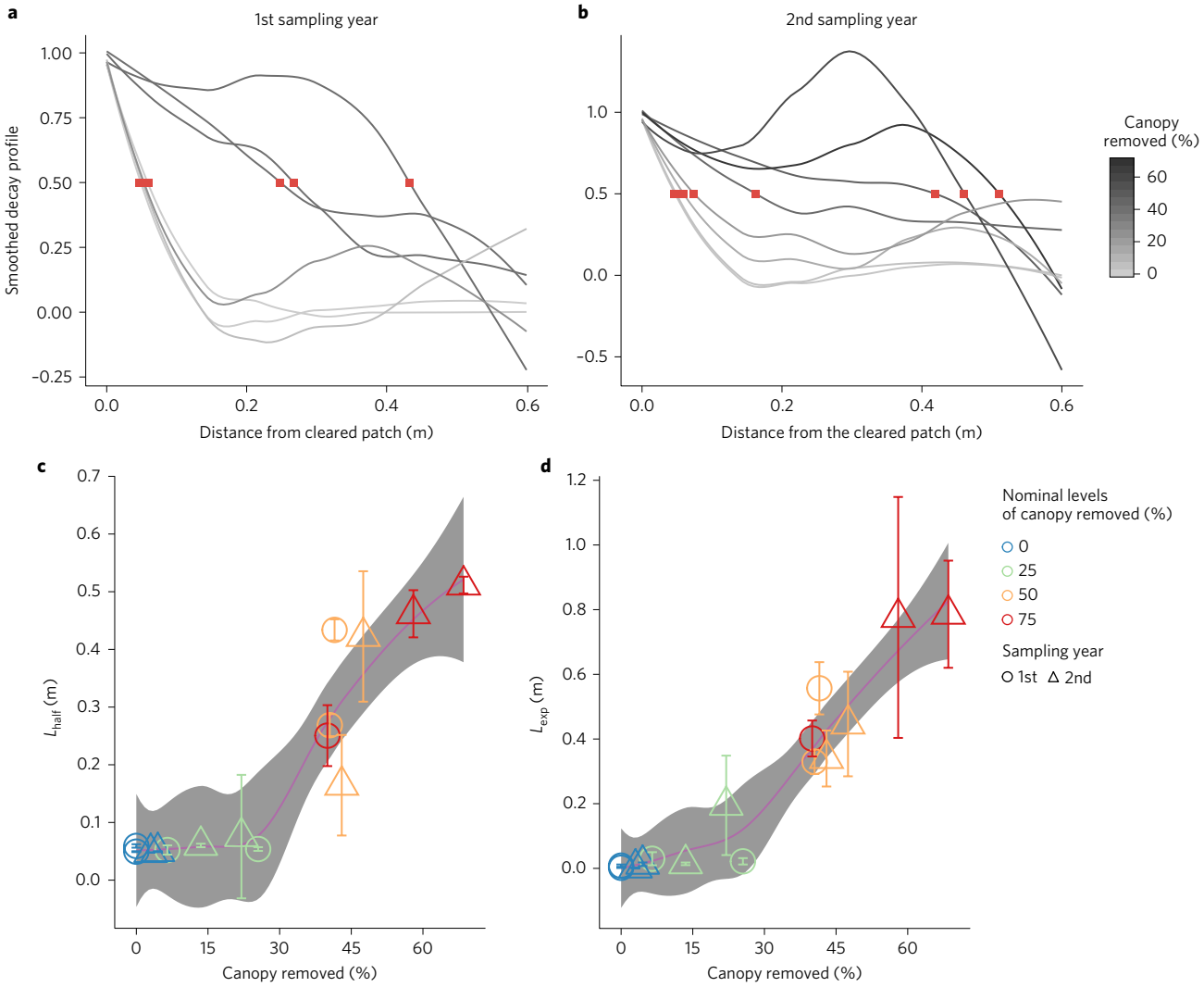

Figure 5 | Recovery length. Two different measurements of recovery length (L_{half} and L_{exp}) increased markedly along the gradient of canopy degradation. **a**,**b**, Smoothed decay profiles of experimental transects for different levels of canopy removed for the first (**a**) and second (**b**) year of sampling. One of two replicate transect of 75% canopy removal treatment of the 1st year was excluded due to high canopy cover in the quadrat adjacent to the cleared patch, which prevented the colonization of algal turfs in that position (Supplementary Fig. 3). Grey colours indicate the percentage of canopy cover removed (expressed as 100 minus observed canopy cover) **c**,**d**, L_{half} and L_{exp}. Errors bars are bootstrapped standard errors. Trends are summarized as LOESS regression lines (in violet) and 95% confidence intervals are shown as shaded areas (in grey).

first two adjacent quadrats in the canopy-degraded region for our analysis. The signal owing to algal turf propagation in quadrats further away from the cleared patch could be masked by algal turf colonization from the water column.

Recovery length. The key metric used in this study to assess recovery in space is the L_{half}[31], which defines the distance at which the cover of algal turfs declines to half of the value observed in the cleared patch. We calculated this metric from the high spatial resolution data, after averaging across the 15 sub-quadrats at a given distance from the cleared patch in each transect. In this way we obtained 30 measurements of turf cover extending 60 cm into the canopy-degraded region at incremental distances of 2 cm from the cleared patch. These measurements were used to define a one-dimensional decay profile of algal turfs. Data were also averaged across all the sub-quadrats in a cleared patch, to obtain a single reference value for each transect. Turf cover was normalized in each decay profile as $z_i = (X_i - X_{31})/(X_1 - X_{31})$, where X_i is an individual measurement of turf cover at position i, whereby i ranges from 1 (the observation in the cleared patch) to 31 (the sub-quadrat extending the furthest into the transect). The L_{half} was estimated by performing a weighted local polynomial regression (R function 'loess', with a span of 0.8) to each decay profile and the location of half-decay, at which $z_{(i=L_{half})} = 0.5z_{i=1}$, was determined (Fig. 5a,b). The span is a parameter that controls the degree of smoothing. We calculated an additional metric to assess recovery in space: L_{exp}, which is the deterministic analogue of L_{half}. L_{exp}, was estimated by fitting a weighted exponential function with two parameters $c_1\exp(-X/L_{exp})$ (R function nlsLM, non-linear least square fitting with Levenberg–Marquardt algorithm) to each decay profile (Supplementary Fig. 6).

One of the two 75% canopy removal transects was excluded from the computation of both indicators (L_{half} and L_{exp}) for the first year, owing to high canopy cover (92%) in the quadrat adjacent to the cleared quality patch, which effectively prevented the invasion of algal turfs in that position. The other 75% canopy removal transect also had more algal canopies than it should in the first year (with about 45% instead of 75% of canopy removed; Fig. 5c,d), but this did not prevent the spread of algal turfs from the cleared patch into the transect. The inability to maintain the nominal level of 75% of algal canopies was a consequence of an unusual recruitment event in the first year of the experiment. Experimental conditions were immediately restored and maintained throughout the second year. These discrepancies increased differences between years for the 75% removal transects. We note, however, that despite differences between nominal and realized treatment levels, the two indicators performed as expected in relation to the amount of algal canopy effectively present in a transect (Fig. 5c,d).

We used bootstrap to calculate the standard errors for both indicators by resampling the measurements 1,000 times for each spatial location x and fitting the average decay profile (Supplementary Methods).

Potential analysis. We used potential analysis to reconstruct the potential landscape of turf cover for different levels of canopy degradation. This analysis used an independent set of data from the data used to quantify recovery length.

© 2017 Macmillan Publishers Limited, part of Springer Nature. All rights reserved.

In July 2013 we established 8 experimental transects as described for the main experiment, but without the cleared patch at one edge, as part of a study on the colonization of alga turfs from the water column. Visual estimates of percentage cover of algal turfs were obtained at high spatial resolution in July 2015, as described for the main experiment.

Potential analysis has been widely applied to highly noisy climate time series and large spatial datasets to test for the presence of alternative states[34]. Assuming that a series of data is approximated by a stochastic potential equation:

$$dZ = -U(z)dt + \sigma dW \quad (1)$$

where $U(z)$ is the potential function, z is the state variable (in our case, percentage algal turf cover measured at the scale of 2 × 2 cm), σ is the magnitude of noise of the system and dW is a noise term (Weiner process), the probability density distribution of the data can be used to calculate the potential landscape of the system, where minima of potential indicate the stable states and maxima the unstable ones. The Fokker–Planck equation allows calculation of the potential (U) from the probability density of the state variable as:

$$U = -\frac{\sigma}{2}\log(p_d) \quad (2)$$

where σ is the magnitude of noise level and p_d is the probability density estimated from experimental data. Notably, as our primary interest was a qualitative estimation of the potential landscape (and identification of stable and unstable states), we scaled the potential to the noise level (U/σ^2). We used a Gaussian kernel to estimate the probability density function with a standard bandwidth estimated by the Scoot's procedure: $h = 1.06s / n^{1/5}$ (where s is the standard deviation of the experimental data and n is the sampling size). The bandwidth was corrected with a factor 0.25 to obtain a more robust estimation of equilibria and to avoid spurious finding due to the discrete nature of the data. Local minima and maxima in the probability density function were numerically estimated, using an optimization procedure, which filters out local patterns when the differences between local maxima and minima were larger than a threshold value (0.005) and with a minimum density of 0.1. Potential analysis was performed using the livpotential_ews function in the earlywarning R package[18,54].

Confidence intervals of turf cover equilibria were obtained by bootstrapping the data of each transect 1,000 times. At each iteration, the potential analysis was applied to data resampled with replacement, and stable and unstable equilibria were estimated and stored. 95% confidence intervals were estimated for each equilibrium as the 2.5th and 97.5th of the bootstrapped data.

Turf–*Cystoseira* model. We developed a simple mathematical model, based on the turf–*Cystoseira* model[10] that included the processes that drive algal turf dynamics in response to canopy loss:

$$\frac{dT}{dt} = rT\left(1 - \frac{T}{K}\right) - CaT\exp^{-bT} + w \quad (3)$$

Here, T is the percentage cover of algal turfs (%), r is the intrinsic growth rate (month^{-1}, hereafter mo^{-1}), K is the percentage carrying capacity (%), C is the percentage cover of *C. amentacea* and w (% mo^{-1}) is the contribution to the benthic cover of algal turfs due to settlement from the water column. The $aT\exp(-bT)$ term models the competitive effect of the canopy on algal turfs, which encapsulates effects due to light attenuation and competition for space. Furthermore, because algal turfs may also colonize from the water column as propagules or spores, we included a density independent influx (w) into the model.

The turf–*Cystoseira* model (Equation (3)) was fitted to unstable and stable equilibrium points of algal turf cover obtained by the potential analysis using maximum-likelihood methods assuming log-normally distributed errors. The predicted stable and unstable equilibria for algal turfs were obtained through a stability analysis repeatedly for each level of the canopy removal treatment[53] (Supplementary Methods). Predicted and observed values of turf cover were compared for maximum-likelihood parameter estimation using function mle2 in the package bbmle assuming log-normally distributed errors[55]. The negative log-likelihood function of equilibrium values of turf cover for a given level of canopy removal (predicted by Equation (1)) is:

$$NLL(T_0(r,\ K,\ a, b,\ w), \sigma_e) = \frac{n}{2}\log(2\pi\sigma_e^2) - \sum_{i=1}^{n}(\log T_{p,i}) - \frac{1}{2\sigma_e^2}\sum_{i=1}^{n}(\log T_{p,i} - \log T_{0,i})^2 \quad (4)$$

where T_o is the predicted equilibrium obtained by the model for a specific level of canopy removed, T_p is the equilibrium (expressed as % turf cover) for a specific value of canopy removed obtained through the potential analysis, σ_e^2 is a parameter that represents the degree of environmental stochasticity, and with the other model parameters as defined for Equation (3). The model was fit to equilibria estimated by the potential analysis (see 'Potential analysis') minimizing the negative log-likelihood function using the Nelder–Mead algorithm (Supplementary Table 1).

To further investigate whether the spatial scale at which the percentage cover of algal turfs decays to zero increases as the system approaches the canopy threshold, we produced a spatial version of the turf–*Cystoseira* model in Equation (3):

$$\frac{\partial T(x,y,t)}{\partial t} = rT\left(1 - \frac{T}{K}\right) - CaTe^{-bT} + w + D\nabla^2 T \quad (5)$$

Vegetative propagation of algal turfs was modelled as Laplace operator

$$\nabla^2 = \left(\frac{\partial^2}{\partial_x^2} + \frac{\partial^2}{\partial_y^2}\right)$$

in x and y spatial coordinates, multiplied by the diffusion coefficient $D = 1 \times 10^{-4}$ m^2 day^{-1}. We did not formally estimate the parameter D using statistical procedures. D coeficient was obtained from a previous study where the colonization of algal turf in cleared patches from *C. amentacea* was monitored for one year[52]. The D coefficient was estimated by dividing the area colonized by algal turf (m^2) by the time needed for the patch to be completely colonized. The model reflects the two-dimensional spatial structure of the experimental transects (Fig. 2) with the cleared patch and the canopy-degraded region embedded within a full canopy of *C. amentacea*. Since the degree of spatial variability in *C. amentacea* cover heavily influences the propagation of algal turfs, we explicitly modelled the spatial heterogeneity in canopy cover[52]. We assumed that *C. amentacea* individuals are approximated by a two-dimensional normal distribution $\mathcal{N}(\mu, \sum)$ where the mean

$$\mu = \begin{pmatrix}\mu_x \\ \mu_y\end{pmatrix}$$

identifies the x and y position in the lattice, and the covariance matrix

$$\sum \begin{pmatrix}\sigma_x^2 & \sigma_x\sigma_y \\ \sigma_x\sigma_y & \sigma_y^2\end{pmatrix}$$

indicates the width of the frond of *C. amentacea*. We set the standard deviations σ_x and σ_y. to 0.2 m, corresponding to the average width of *C. amentacea* fronds.

We further explored the response L_{half} and L_{exp} to canopy degradation by computing these spatial indicators from the spatial model. Therefore, we generated 100 random spatial patterns of canopy cover and ran the model for each level of canopy removal. We then computed L_{half} and L_{exp} for each simulated transect and obtained means and standard errors of indicators over the 100 replicates. Spatial model simulations were carried out using: raster[56], mvtnorm[57], deSolve[58], ReacTran[59] R packages.

Code availability. R scripts used to conduct the Maximum-likelihood estimation, bootstrap analysis and model simulations can be found at: https://figshare.com/s/2eecbb7327adb7fc2d97.

Data availability. Data used in this study can be found at following link: https://figshare.com/s/2eecbb7327adb7fc2d97.

Received 16 June 2016; accepted 24 March 2017; published 8 May 2017

References

1. Scheffer, M., Carpenter, S., Foley, J. A., Folke, C. & Walker, B. Catastrophic shifts in ecosystems. *Nature* **413,** 591–596 (2001).
2. Hughes, T. P. Catastrophes, phase shifts, and large-scale degradation of a Caribbean coral reef. *Science* **265,** 1547–1551 (1994).
3. Staver, A. C., Archibald, S. & Levin, S. A. The global extent and determinants of savanna and forest as alternative biome states. *Science* **334,** 230–232 (2011).
4. Wissel, C. A universal law of the characteristic return time near thresholds. *Oecologia* **65,** 101–107 (1984).
5. Scheffer, M. *et al.* Anticipating critical transitions. *Science* **338,** 344–348 (2012).
6. Scheffer, M. *et al.* Early-warning signals for critical transitions. *Nature* **461,** 53–59 (2009).
7. van Nes, E. H. & Scheffer, M. Slow recovery from perturbations as a generic indicator of a nearby catastrophic shift. *Am. Nat.* **169,** 738–747 (2007).
8. Dai, L., Vorselen, D., Korolev, K. S. & Gore, J. Generic indicators for loss of resilience before a tipping point leading to population collapse. *Science* **336,** 1175–1177 (2012).
9. Veraart, A. J. *et al.* Recovery rates reflect distance to a tipping point in a living system. *Nature* **481,** 357–359 (2012).
10. Benedetti-Cecchi, L., Tamburello, L., Maggi, E. & Bulleri, F. Experimental perturbations modify the performance of early warning indicators of regime shift. *Curr. Biol.* **25,** 1867–1872 (2015).

© 2017 Macmillan Publishers Limited, part of Springer Nature. All rights reserved.

11. Carpenter, S. R. *et al.* Early warnings of regime shifts: a whole-ecosystem experiment. *Science* **332,** 1079–1082 (2011).
12. Cline, T. J. *et al.* Early warnings of regime shifts: evaluation of spatial indicators from a whole-ecosystem experiment. *Ecosphere* **5,** 1–13 (2014).
13. Drake, J. M. & Griffen, B. D. Early warning signals of extinction in deteriorating environments. *Nature* **467,** 456–459 (2010).
14. Dakos, V. *et al.* Slowing down as an early warning signal for abrupt climate change. *Proc. Natl Acad. Sci. USA* **105,** 14308–14312 (2008).
15. Lade, S. J. & Gross, T. Early warning signals for critical transitions: a generalized modeling approach. *PLoS Comput. Biol.* **8,** e1002360 (2012).
16. Kéfi, S., Dakos, V., Scheffer, M., Van Nes, E. H. & Rietkerk, M. Early warning signals also precede non-catastrophic transitions. *Oikos* **122,** 641–648 (2013).
17. Boettiger, C. & Hastings, A. Early warning signals and the prosecutor's fallacy. *Proc. R. Soc. B* **279,** 4734–4739 (2012).
18. Dakos, V. *et al.* Methods for detecting early warnings of critical transitions in time series illustrated using simulated ecological data. *PLoS ONE* **7,** e41010 (2012).
19. Bestelmeyer, B. T. *et al.* Analysis of abrupt transitions in ecological systems. *Ecosphere* **2,** 1–26 (2011).
20. Lenton, T. M., Livina, V. N., Dakos, V., van Nes, E. H. & Scheffer, M. Early warning of climate tipping points from critical slowing down: comparing methods to improve robustness. *Phil. Trans. R. Soc. A* **370,** 1185–1204 (2012).
21. Kefi, S. *et al.* Early warning signals of ecological transitions: methods for spatial patterns. *PLoS ONE* **9,** e92097 (2014).
22. Dakos, V., van Nes, E. H., Donangelo, R., Fort, H. & Scheffer, M. Spatial correlation as leading indicator of catastrophic shifts. *Theor. Ecol.* **3,** 163–174 (2010).
23. Guttal, V. & Jayaprakash, C. Spatial variance and spatial skewness: leading indicators of regime shifts in spatial ecological systems. *Theor. Ecol.* **2,** 3–12 (2000).
24. Streeter, R. & Dugmore, A. J. Anticipating land surface change. *Proc. Natl Acad. Sci. USA* **110,** 5779–5784 (2013).
25. Litzow, M. A., Urban, J. D. & Laurel, B. J. Increased spatial variance accompanies reorganization of two continental shelf ecosystems. *Ecol. Appl.* **18,** 1331–1337 (2008).
26. Carpenter, S. R. & Brock, W. A. Early warnings of regime shifts in spatial dynamics using the discrete Fourier transform. *Ecosphere* **1,** 1–15 (2010).
27. Kefi, S. *et al.* Spatial vegetation patterns and imminent desertification in Mediterranean arid ecosystems. *Nature* **449,** 213–217 (2007).
28. Kefi, S. *et al.* Robust scaling in ecosystems and the meltdown of patch size distributions before extinction. *Ecol. Lett.* **14,** 29–35 (2011).
29. Rietkerk, M., Dekker, S. C., de Ruiter, P. C. & van de Koppel, J. Self-organized patchiness and catastrophic shifts in ecosystems. *Science* **305,** 1926–1929 (2004).
30. Dakos, V., Kefi, S., Rietkerk, M., van Nes, E. H. & Scheffer, M. Slowing down in spatially patterned ecosystems at the brink of collapse. *Am. Nat.* **177,** E153–E166 (2011).
31. Dai, L., Korolev, K. S. & Gore, J. Slower recovery in space before collapse of connected populations. *Nature* **496,** 355–358 (2013).
32. Dai, L., Korolev, K. S. & Gore, J. Relation between stability and resilience determines the performance of early warning signals under different environmental drivers. *Proc. Natl Acad. Sci. USA* **112,** 10056–10061 (2015).
33. Scheffer, M., Carpenter, S. R., Dakos, V. & van Nes, E. H. Generic indicators of ecological resilience: inferring the chance of a critical transition. *Annu. Rev. Ecol. Evol. Syst.* **46,** 145–167 (2015).
34. Livina, V. N., Kwasniok, F. & Lenton, T. M. Potential analysis reveals changing number of climate states during the last 60 kyr. *Clim. Past* **6,** 77–82 (2010).
35. Konar, B. & Estes, J. A. The stability of boundary regions between kelp beds and deforested areas. *Ecology* **84,** 174–185 (2003).
36. Robles, C. D., Garza, C., Desharnais, R. A. & Donahue, M. J. Landscape patterns in boundary intensity: a case study of mussel beds. *Landscape Ecol.* **25,** 745–759 (2010).
37. Scheffer, M. *et al.* Vegetated areas with clear water in turbid shallow lakes. *Aquat. Bot.* **49,** 193–196 (1994).
38. Silliman, B. R., van de Koppel, J., Bertness, M. D., Stanton, L. E. & Mendelssohn, I. A. Drought, snails, and large-scale die-off of southern U.S. salt marshes. *Science* **310,** 1803–1806 (2005).
39. Da Silveira Lobo Sternberg, L. Savanna–forest hysteresis in the tropics. *Global Ecol. Biogeogr.* **10,** 369–378 (2001).
40. Batt, R. D., Carpenter, S. R., Cole, J. J., Pace, M. L. & Johnson, R. A. Changes in ecosystem resilience detected in automated measures of ecosystem metabolism during a whole-lake manipulation. *Proc. Natl Acad. Sci. USA* **110,** 17398–17403 (2013).
41. Rietkerk, M. & van de Koppel, J. Regular pattern formation in real ecosystems. *Trends Ecol. Evol.* **23,** 169–175 (2008).
42. Barbier, N., Couteron, P., Lejoly, J., Deblauwe, V. & Lejeune, O. Self-organized vegetation patterning as a fingerprint of climate and human impact on semi-arid ecosystems. *J. Ecol.* **94,** 537–547 (2006).
43. Steneck, R. S. *et al.* Kelp forest ecosystems: biodiversity, stability, resilience and future. *Environ. Conserv.* **29,** 436–459 (2002).
44. Benedetti-Cecchi, L. *et al.* Predicting the consequences of anthropogenic disturbance: large-scale effects of loss of canopy algae on rocky shores. *Mar. Ecol. Prog. Ser.* **214,** 137–150 (2001).
45. Connell, S. D. *et al.* Recovering a lost baseline: missing kelp forests from a metropolitan coast. *Mar. Ecol. Prog. Ser.* **360,** 63–72 (2008).
46. Beck, M. & Airoldi, L. Loss, status and trends for coastal marine habitats of Europe. *Oceanogr. Mar. Biol.* **45,** 345–405 (2007).
47. Pace, M. L., Carpenter, S. R. & Cole, J. J. With and without warning: managing ecosystems in a changing world. *Front. Ecol. Environ.* **13,** 460–467 (2015).
48. Lenton, T. M. & Williams, H. T. On the origin of planetary-scale tipping points. *Trends Ecol. Evol.* **28,** 380–382 (2013).
49. Brook, B. W., Ellis, E. C., Perring, M. P., Mackay, A. W. & Blomqvist, L. Does the terrestrial biosphere have planetary tipping points? *Trends Ecol. Evol.* **28,** 396–401 (2013).
50. Worm, B. & Lotze, H. K. Effects of eutrophication, grazing, and algal blooms on rocky shores. *Limnol. Oceanogr.* **51,** 569–579 (2006).
51. Benedetti-Cecchi, L. *et al.* Linking patterns and processes across scales: the application of scale-transition theory to algal dynamics on rocky shores. *J. Exp. Biol.* **215,** 977–985 (2012).
52. Tamburello, L., Bulleri, F., Bertocci, I., Maggi, E. & Benedetti-Cecchi, L. Reddened seascapes: experimentally induced shifts in 1/fspectra of spatial variability in rocky intertidal assemblages. *Ecology* **94,** 1102–1111 (2013).
53. Connell, S. D., Foster, M. S. & Airoldi, L. What are algal turfs? Towards a better description of turfs. *Mar. Ecol. Prog. Ser.* **495,** 299–307 (2014).
54. Lahti, L., Salojärvi, J., Salonen, A., Scheffer, M. & de Vos, W. M. Tipping elements in the human intestinal ecosystem. *Nat. Commun.* **5,** 4344 (2014).
55. Bolker, B. M. *Ecological Models and Data in R*. (Princeton Univ. Press, 2008).
56. Hijmans, R. J. & van Etten, J. raster: geographic analysis and modeling with raster data, R package version 2.0-12. (2012).
57. Genz, A. & Bretz, F. *Computation of Multivariate Normal and t Probabilities.* (Springer Berlin Heidelberg, 2009).
58. Soetaert, K., Cash, J. & Mazzia, F. *Solving Differential Equations in R.* (Springer Berlin Heidelberg, 2012).
59. Soetaert, K. & Meysman, F. Reactive transport in aquatic ecosystems: rapid model prototyping in the open source software R. *Environ. Model. Softw.* **32,** 49–60 (2012).

Acknowledgements

We thank E. Maggi, F. Bulleri, C. Ravaglioli and L. Tamburello for field and technical assistance, A. Rattray for useful comments on the manuscript, A. Perez-Escudero for helping to develop the model, R. Casagrandi and L. Mari for their feedback. The authors acknowledge financial support from University of Pisa through the PRA (PRA_2015_055) and MISTI projects, the latter in collaboration with MIT. J.G. also acknowledges support from an NIH New Innovator Award (DP2 AG044279).

Author contributions

L.R. and L.B.-C. designed the study. L.R. did the analyses and wrote the first draft of the manuscript. M.D.B., L.D. and J.G. assisted with the analysis. L.R., M.D.B and L.B.-C. performed the experiment. All authors contributed to interpreting the results and commented on the manuscript.

Additional information

Supplementary information is available for this paper.

Reprints and permissions information is available at www.nature.com/reprints.

Correspondence and requests for materials should be addressed to L.R.

How to cite this article: Rindi, L., Dal Bello, M., Dai, L., Gore, J. & Benedetti-Cecchi, L. Direct observation of increasing recovery length before collapse of a marine benthic ecosystem. *Nat. Ecol. Evol.* **1,** 0153 (2017).

Publisher's note: Springer Nature remains neutral with regard to jurisdictional claims in published maps and institutional affiliations.

Competing interests

The authors declare no competing financial interest.

© 2017 Macmillan Publishers Limited, part of Springer Nature. All rights reserved.